An- Najah National University

Faculty of Engineering

Chemical Engineering Department

Graduation project II (10626594)

Carbon Nanodots from Olive Solid Wastes for Photodegradation of Methylene Blue

Prepared by:

Halah Azzam

Hanan Dweikat

Kayan Anaya

Rasha Bin Ali

Supervised by:

Dr. Shadi Sawalha

This project was submitted in partial fulfillment of the requirements of the degree of Bachelor in Chemical Engineering

May 23, 2021

Statement of Originality

We, the undersigned, hereby declare that this work (Graduation project entitled Carbon Nanodots from Olive Solid Wastes for Photodegradation of Methylene Blue) has not previously been submitted for a degree or diploma at any university or institute. To the best of our knowledge and belief, the thesis contains no material previously published or written by another person's except where due reference is indicated in the thesis itself.

Halah Azzam

Hanan Dweikat

Kayan Anaya

Rasha Bin Ali

May 23, 2021

Abstract

Carbon dots are emerging materials in the nanotechnology field as attractive photocatalysts, owing to their high water-solubility, good chemical and photostability, tunable photoluminescence and photoinduced phenomena.

CQDs were synthesized from olive solid waste by pyrolyzing the waste at 600 °C followed by a chemical oxidation in the presence of hydrogen peroxide. The synthesized CQDs were utilized in this work as photocatalysis for the photodegradation of methylene blue at different conditions, such as; the catalyst concentration, pH of the pollutant solution (M.B), salt content, light source distance, source of light and pollutant concentration (M.B).

The degradation efficiency and rate were studied for all aforementioned factors, finding that the increase in the CQDs dose into the M.B solution increases linearly both the efficiency and the rate. On the other hand, the maximum degradation rate was observed at pH = 10.6 with an efficiency of 92% after 120 minutes of irradiation.

Moreover, the existence of NaCl salt in the pollutant solution affects adversely the degradation parameters showing a slight decrease in degradation rate, each 2 mg addition decreased the rate with less than 1.2 folds.

The potential and the distance of the visible light source from the pollutant cell have an obvious effect on the degradation, increasing the light power from 10 to 50 W, increased the degradation rate 16 times.

Besides the use of CQDs as photocatalysts in solutions, a CQDs/ZnO nanocomposite was prepared and the photodegradation of M.B was also tested showing an enhancement due to the addition of CQDs. For instance, the degradation rate was increased about 2 folds.

Table of Contents

List of Figures:

List of Tables:

Chapter One: Introduction

Carbon quantum dots (CQDs) are small nano-sized carbon nano-materials, were first synthesized from carbon nanotubes (CNTs) during the process of electrophoresis[1], having internal sp^2 and external sp^3 carbon atoms[2]. The CQDs are rich in hydrophilic functional groups, such as carboxyl, hydroxyl, amino and so on, which can be uniformly dispersed in polar solvents [3]. CQDs are exhibits unique chemical and physical properties such as luminescent property, chemical inertness, low toxicity, excellent water solubility and conductivity[4]. They have been used for various applications, such as sensors, bio-imaging, electrogenerated chemiluminescence, solar to fuel production [5], photocatalyst for degradation of pollutants [6].

The strategy for synthesizing CQDs includes pyrolytic decomposition or carbonization [7], chemical oxidation [8], arc discharge [9], laser etching [10], electrochemistry [11], microwave [12] and hydrothermal methods [13]. Importantly, the hydrothermal technique is widely used because to its simple procedure, excellent controllability, high purity, and environmentally benign products [13].

One of the most important applications of CQDs is photocatalytic processes which require efficient charge transfer in photocatalytic materials [14], and CQDs with electron-trapping ability can easily capture photogenerated electrons from the materials [15]. This allows effective separation of photogenerated electron–hole pairs. Considering their effects in photocatalysis process [16]. Also, CQDs can be coupled with other nano materials such as ZnO and form nanocomposites that are used as photocatalysts [17].

Synthetic organic dyes are commonly used in various industries, such as in textiles, leather, dyes, foods and cosmetics [18, 19]. They are one of the main water pollutants that can be a major threat to aquatic life [18, 19].The most commonly used dye in textile industries is methylene blue, which is used for dyeing and cloth completion processes [20]. However, excessive exposure to methylene blue is harmful to human and aquatic life as it can cause skin allergies, dermatitis, nervous system disorders, and ultimately cardiovascular damages [21, 22].

CQDs have excellent photo-luminescent properties in which they can convert visible light to a shorter wavelength that can extend the wide band-gap of a semiconductor [23]. CQDs is good for trapping and transferring electrons. Hence, CQDs can be one of

the best candidates in the photocatalytic degradation of organic dyes (M.B) [20]. Photo-catalysis is an energy conversion process of semiconductor materials that can be initiated by light absorption. During photo-catalysis, electrons and holes can be generated by light exposure [24]. CQDs can be considered to be good photo-catalysts in the degradation of organic dyes owing to their strong visible-light absorption, excellent light-trapping ability, and high efficiency in the separation of photo-generated charge carriers [20].

The photodegradation efficiency of the pollutant within the presence of CQDs as photocatalysts is affected by several factors, which can play a big role in the time required to obtain the best degradation rate of the pollutant. Among the most important of these factors are pH [25], salt concentrations [26], concentrations of pollutant [27], concentrations of photocatalyst [27], source of light [28], distance of light [28].

In this work, CQDs synthesized from olive solid waste as cheap and abundant precursor will be used as a photocatalyst in order to remove organic pollutants such as methylene blue from water. Different factors that may affect the M.B photodegradation process will be studied. These factors are the photocatalyst dose, pH, pollutant concentration, source potential and location in addition to the salt content. Photodegradation efficiency and rate will be the most parameters to monitored. Furthermore, CQDs/ZnO nanocomposite will be prepared to study the photodegradation process and the benefit of combining these two components.

Chapter Two: Photocatalysis

In general, photocatalysis is the activity occurring when a light source interacts with the surface of semiconductor materials, the acceleration of a photoreaction in the presence of a catalyst, the so called photocatalysts. The most important thing that distinguishes it is very attractive and currently in high demand. Since it provides a clean and cost-effective method for the water purification. Additionally, visible light driven photocatalysis offers to employ renewable and abundant energy to promote dye degradation under mild conditions [29].

Photocatalysis is one of the most important applications of CQDs. The thrust of this project is the application of CQDs as photocatalysts in the degradation of M.B, where it includes occurrence of at least two simultaneous interactions, oxidation from photogenerated holes and reduction from photogenerated electrons [30].

The following is a detailed explanation of the mechanism by which the pollutant is degraded. When photons of appropriate energy fall on CQDs, electrons were excited from the initial state (valence band) to the excitation state (conduction band), generating excess electrons (e^-) and holes (h^+). Due to the rich presence of surface defects, because of the presence of the functional groups on the surface of CQDs, some of the excited carriers are trapped, and the recombination of e- and h+ are hampered. As a result, the pollutant (M.B) could be oxidized by the h+ directly to cause the degradation. Where after this reaction occurs (photocatalysts degradation), the products appear in the form of water and carbon dioxide, and this depends on several things, the most important of which are the time that the photocatalysts were exposed to light and the amount of incident light itself [31]. See Fig. (2-1).

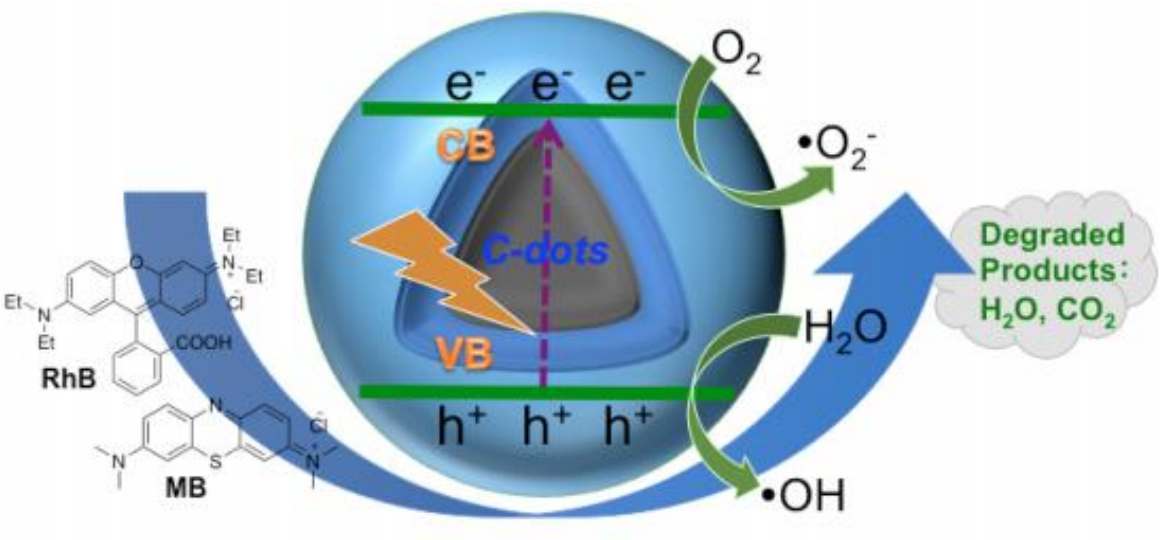

Figure (2-1): Mechanism of the photocatalytic degradation of M.B [31].

Moreover, a comprehensive review was conducted with regard to the photocatalysis applications of CQDs and summarized in table A1 in appendix, it consists of the source of CQDs, their synthesis methods, photocatalysis application and the produced size. In addition to the role of CQDs in improving the photocatalysis activity.

Chapter Three: Experimental Work

Experimental work can be divided into three parts:

3.1 Synthesis of CQDs

CQDs were prepared from olive solid waste (OSWs) according to the Sawalha et al. protocol [32]. The preparation method began by drying the OSWs at 105 °C for a period ranging from 3 to 4 hours, and then they were carbonized at a temperature of 600 °C for a 1 hour. The carbonized OSWs were grinded into fine powder where 100 mg were dispersed in 10 ml of deionized water contained 150 µl of 30% hydrogen peroxides. The mixture was sonicated 10 min and then refluxed at 100 °C for 90 min. The reaction products were cooled to room temperature and centrifuged at 3900 rpm for half an hour. After that the supernatant was filtered through 0.2 µm syringe filter. The synthesis procedure is illustrated in Fig. (3-2).

Figure (3-2): Steps for synthesis of CQDs.

3.2 Characterizations of CQDs

The Thermo Scientific™ GENESYS™ 10S UV-Vis Spectrophotometer was used to record the UV-Vis spectra of CQDs solution from 800 to 200 nm. It was also used to investigate the maximum absorption peak of M.B solution. The same instrument was utilized to record the UV-Vis absorption for the solution of M.B-CQDs after light irradiation for 120 min with 10 min increment.

3.3 CQDs/ZnO nanocomposite preparation

CQDs/ZnO composite nanoparticles were prepared by dispersing 5 mg of ZnO in 2 ml (0.04 mg/ml CQDs) the solution was left for 48 hours, and then dried at 80 °C for 24 hours. The result was a nanocomposite in the form of a white powder.

3.4 Photodegradation Experiments

3.4.1 Preparation of Methylene blue solution

Methylene blue solution was prepared by dissolving the M.B powder in deionized water, the mother solution had 35µM concentration. The maximum absorption peak of M/B solution was obtained by conduction a UV-Vis absorption scan in the range of 800 – 200 nm.

3.4.2 Photodegradation

- 500 µl of CQDs (0.0.04 mg/ml) were added into 3 ml of M.B (35 µM), the solution was left for 2 hours in dark to examine whether or not the addition of CQDs will act as a catalyst.
- 35 µM of M.B solution with absence and presence of CQDs were subjected to yellow visible light of 50 W for a duration of 120 min. The concentration of CQDs as a photocatalyst dose was altered through adding 200, 300, 400 and 500 µl of 0.04 mg/ml of CQDs, obtaining final concentrations of 0.267, 0.4, 0.53, and 0.667 mg/l of carbon dots in M.B solution. Before light irradiation, all solution were left for half an hour to obtain an absorption-desorption equilibrium between solution species. The UV-Vis absorption was recorded for each sample at 613 nm (M.B maximum absorption peak) at 10 minutes increment. The same irradiation procedures were carried out for all experiments.
- The effect of the pH on photodegradation process has been studied at values (3.8, 7, 10.6) by adding some drops of 1 molar of sodium hydroxide and hydrochloric solutions and similar procedure of light irradiation was followed to observe the effect of pH on M.B photodegradation.
- Sodium hydroxide (NaCl) effect was also carried out by adding different amounts (2, 4, 8) mg to 3 ml M.B solution.
- The effect of distance between the light source and the pollutant (M.B) on photodegradation has been investigated. 5 & 10 cm distances have been selected.

- Different powers 50 and 10 watt were used to obtain the effect of the source of light.
- Three amounts of pollutant (35, 23.33, 17.5) μM of M.B were adjusted to study the effect of pollutant amount on photodegradation process.

Chapter Four: Results and Discussion

CQDs was easily fabricated by top-down route using pyrolysis and chemical oxidation method from olive solid wastes and hydrogen peroxide. 0.8 mg/L CQDs solution of yellowish color has been obtained. The resulting CQDs was tested by UV-vis and gave the curve that shown in Fig. (4-3), which is identical to the other carbon quantum dots [32].

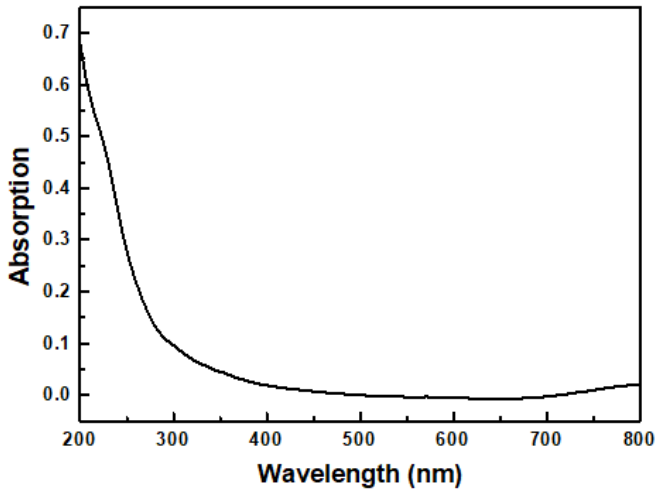

Figure (4-3): UV-Vis's absorption spectrum of CQDs.

To test whether CQDs will act as catalysts or photocatalysts, equal amount of CQDs were spiked into M.B solution, one of them was left in dark and the other one was irradiated for 120 min. Every 10 minutes the UV-Vis absorption at 613 was recorded and the degradation efficiency was evaluated and plotted versus time as in Figure (4-4).

Without light irradiation, CQDs are not active and could not behave as catalyst, while under light CQDs are active and lead to photodegrade M.B proving that they could be considered as photocatalysts. See Fig. (4-5).

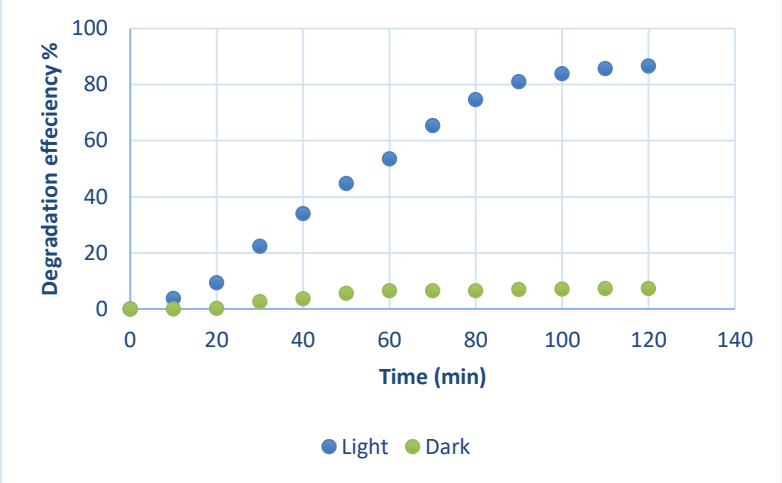

Figure (4-4): Role of CQDs in dark Vs light irradiation.

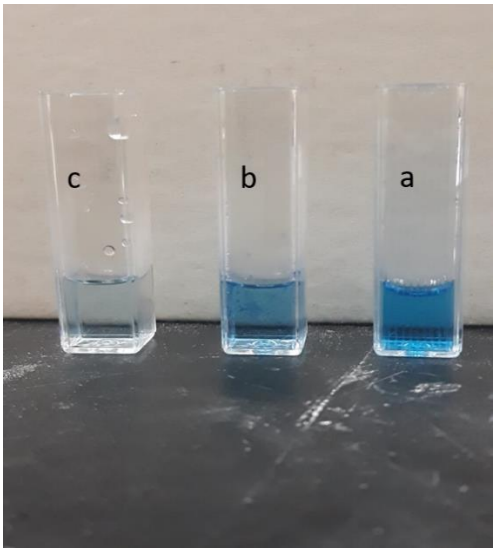

Figure (4-5): Degradation of: a) M.B alone in dark ; b) M.B under light irriadation; M.B with CQDs under light irriadation.

Many factors may affect the photodegradation process of M.B, the effect factors are as follows:

4.1 Effect of Dose of Photocatalyst on Degradation.

The degradation of methylene blue in the presence of different amounts of CQDs was investigated, the concentration of the CQDs (Dose) was changed (0, 0.267, 0.4, 0.53, 0.667 mg/l) and table A2 in appendix. The degradation efficiency of M.B was plotted versus the CQDs dose in Fig. (4-5). As illustrated in the Figure the degradation efficiency at 120 min is increased from 27.4% for M.B in the absence of the photocatalyst up to 86.5% in the presence of CQDs with 0.667 mg/l [28].

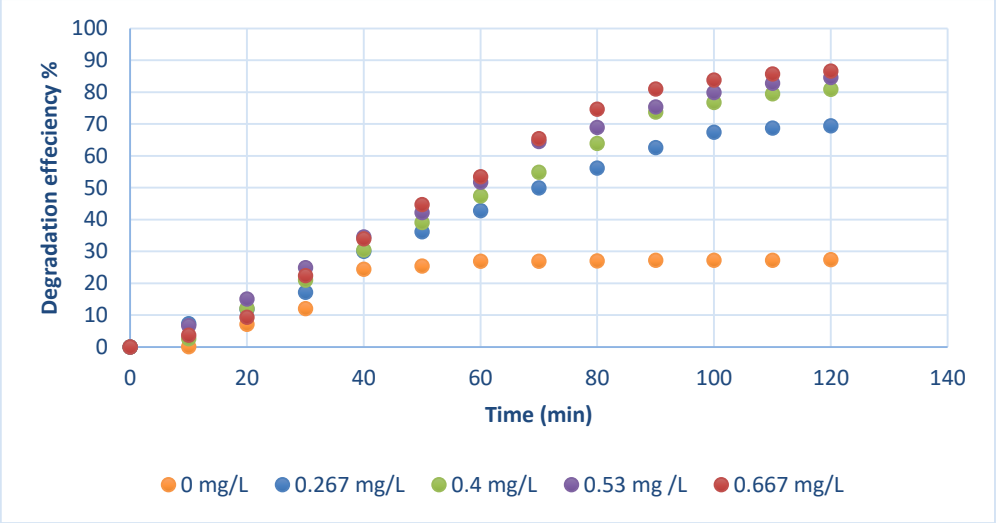

Figure (4-6): Effect of CQDs doses on degradation of M.B.

Where the M.B degradation efficiency (or degree of degradation) could be reflected by the UV-Vis absorption changes of the M.B and calculated according to the following equation:

$$\text{Degradation effeciency} = \frac{\text{Co} - \text{C}}{\text{Co}} \times 100\%$$

where Co represents the absorbance of M.B at time zero, and C is the absorbance of M.B after degradation. And according to the Langmuir–Hinshelwood dynamic model [28], the degradation kinetics of M.B could be simplified according to the pseudo first-order kinetic equation below if the dye solution is very dilute:

$$\ln\left(\frac{\text{Co}}{\text{C}}\right) = \text{k} \times \text{t}$$

Where Co and C should be the equilibrium concentration of M.B and the concentration of M.B after irradiation time t, respectively. For calculation purposes, here, Co and C are taken as the absorbance of the dyes at time zero and the absorbance of the dyes after degradation time t, respectively; k stands for the dye degradation rate constant as shown in Fig. (4-6).

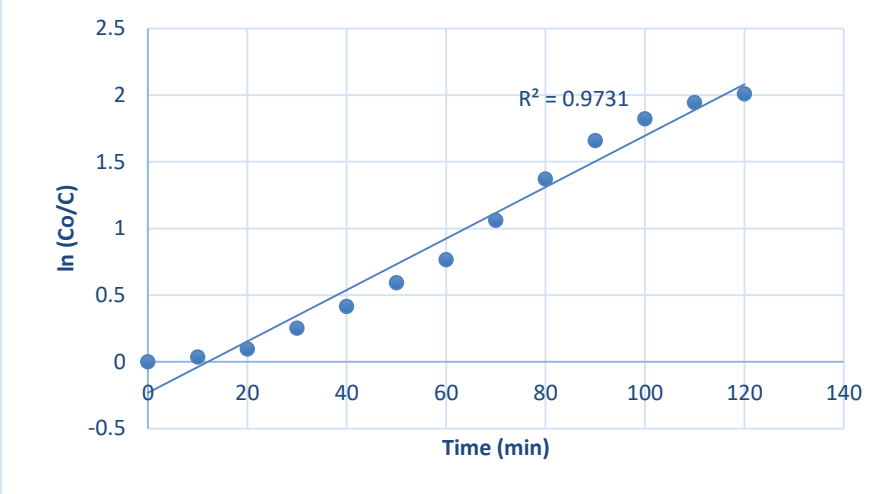

Figure (4-7): Irradiation time-dependent pseudo first-order kinetics plot (ln (Co /C) vs. time) of M.B.

The increase of CQDs dose means increasing in active (catalyst) sites, and this led to increase in degradation rate of M.B as illustrated in Fig. (4-7).

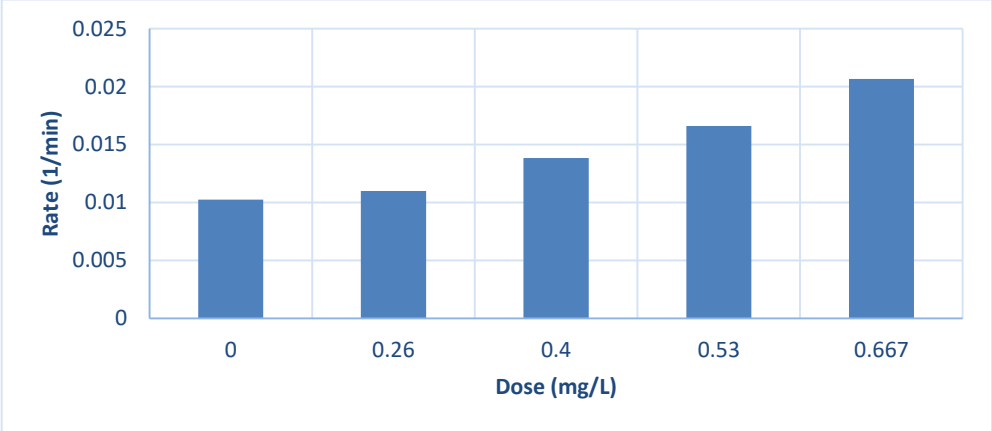

Figure (4-8): Dose of CQDs vs. degradation rate.

According to the results and discussions above, a plausible photocatalytic mechanism for dye degradation under the catalysis of (CQDs) is proposed (Fig. 4-8). When photons of appropriate energy excite C-dots, electrons were excited from the ground state (valence band) to excitation state (conduction band), generating excess electrons (e−) and holes (h+). Due to the rich presence of surface defects on C-dots, some of the excited carriers are trapped, and the recombination of e- and h+ are hindered. As a result, the methylene blue could be oxidized by the h+ directly to cause the degradation, [33]. In the meantime, some of the e− could be captured by oxygen dissolved in the solution, forming super oxide radicals, some of the h+ could interact with surface-

adsorbed H_2O to form hydroxyl radicals. Reactive oxygen species (ROS) , super oxide [34] and hydroxyl radical [33, 35]are known to degrade organic dyes.

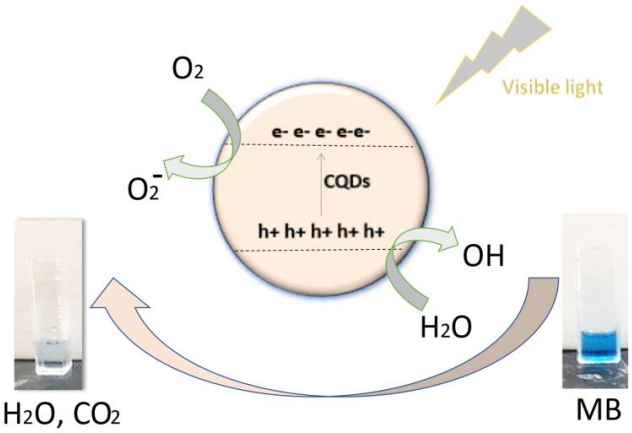

Figure (4-9): Mechanism of degradation of M.B.

4.2 Effect of pH on Degradation of M.B

In general, pH was considered to be a critical role during the photocatalytic process. As it impacts the surface charges of photocatalysts, electrostatic interactions between the pollutants and the photocatalysts, the formation of pollutant and the ionization states of M.B [36]. Fig. (4-9) and table A3 in appendix show the degradation efficiency at different values of pH, the best efficiency of degradation of M.B was at pH=10.6 (base condition) to be 91.2%, with degradation rate 0.0606 1/min as shown in Fig. (4-10).

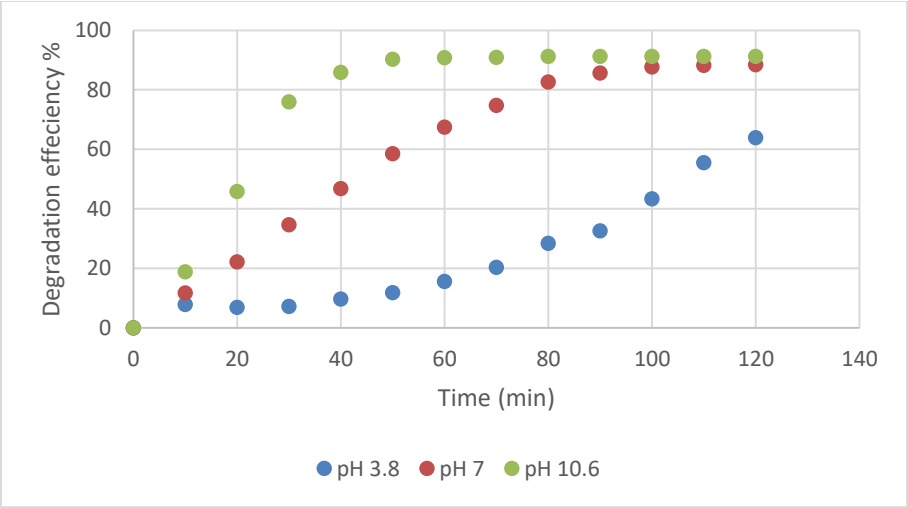

Figure (4-10): Effect of pH on degradation of M.B by CQDs.

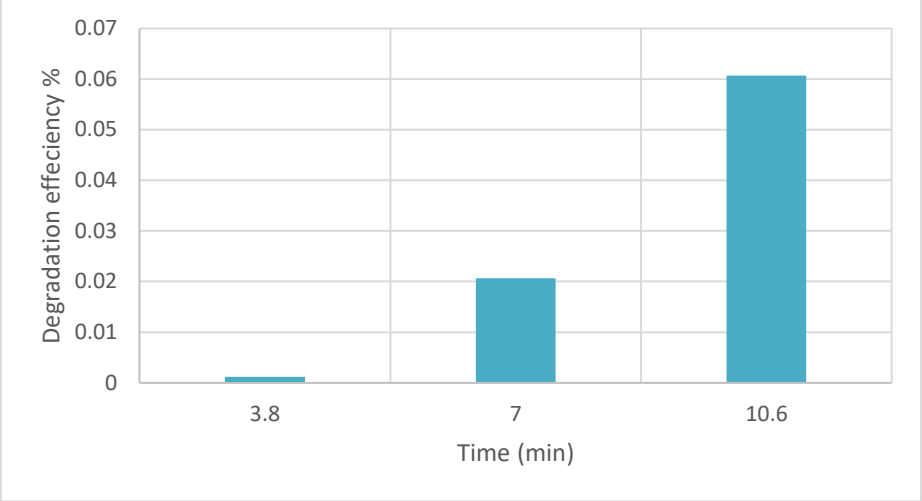

Figure (4-11): Degradation rate at different pH values.

These results could be ascribed to the increase in negativity (anionic) of CQDs [28] as Zeta-potential decreased from -26.7 eV at pH=3 (acid condition) to -32 eV on pH =7.4, this change in negativity could be related to increase in hydroxyl surface groups which in their turn act as surface traps causing more hindering of e- and h+ recombination [32].

4.3 Effect of Salts Concentration

Sodium chloride was added to the pollutant solution (M.B) to explore its influence on the degradation process. Figures (4-10) & (4-11) display the degradation curves of M.B under four different concentrations of NaCl salt (0, 2, 4, 8) in mg/ml. See table A4 in appendix.

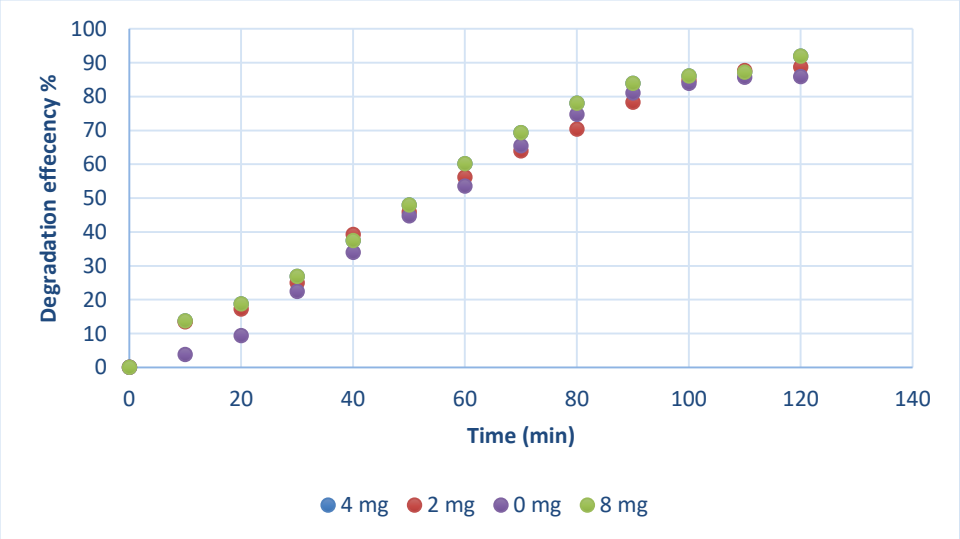

Figure (4-12): Effect of NaCl ions on M.B photodegradation performance by CQDs under visible light irradiation.

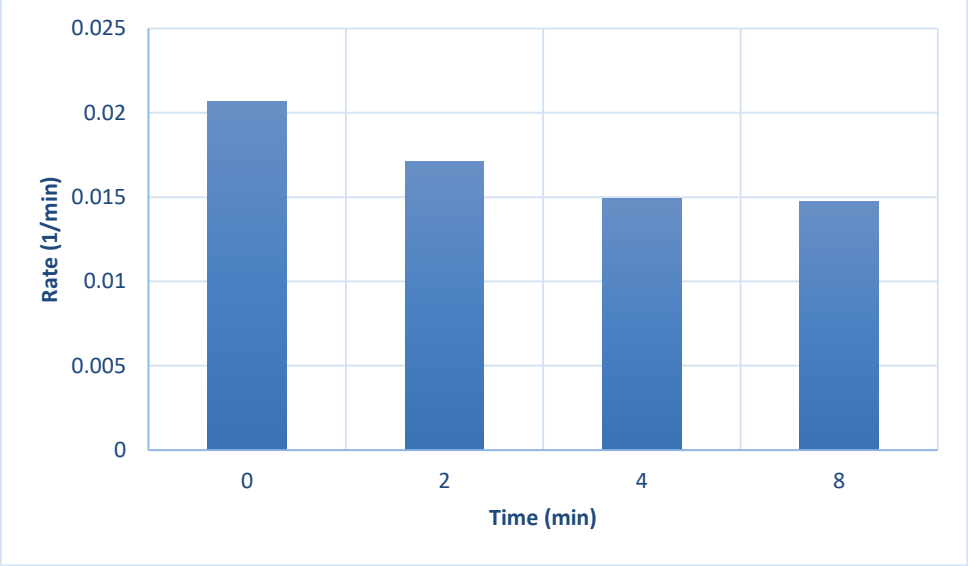

Figure (4-13): Degradation rate at different concentrations of NaCl ion.

The addition of salt decreases the degradation rate of M.B (Fig. 4-11). In this case NaCl salt behaves as a suppressing agent impedes slightly the generation of e- and h+ after excitation from the ground state [26].

4.4 Effect of Distance of light irradiation

The distance of the light source from the pollutant was changed from 10 cm to 5 cm, this proximity causes an improvement in degradation efficiency as shown in Fig. (4-12) also an increase in degradation rate from 0.02067 to 0.02435 1/min was obtained. The closeness of light results in much more incident photons onto the CQDs surface causing more or fast generation of holes and electrons upon excitation. See table A5 in appendix.

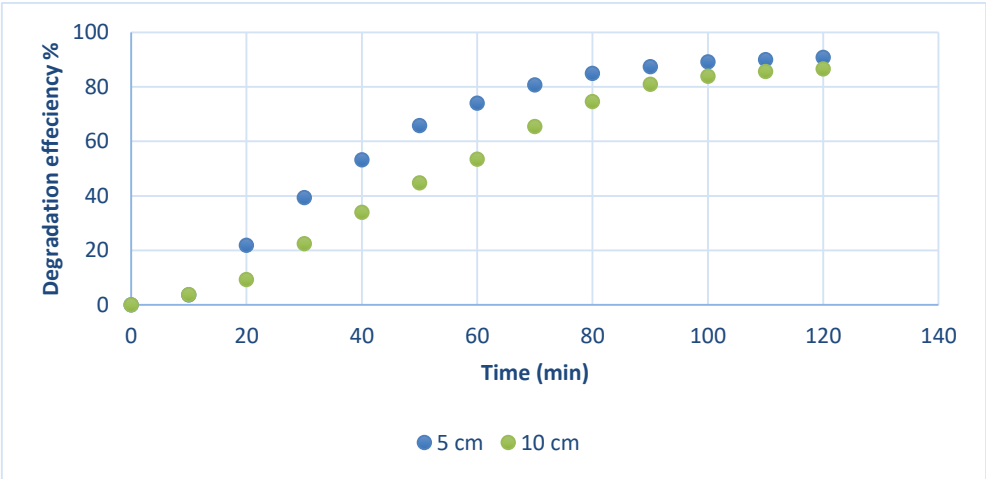

Figure (4-14): Effect of distance on M.B photodegradation performance by CQDs under visible light irradiation.

4.5 Effect of Light Source on Photodegradation

Photocatalytic phenomena rely on the energy supplied by light quanta. Electron–hole pairs are generated in the conduction band and valance band of a photocatalytic material when they receive photons with energy equal to or greater than the band gap of the material. The light intensity plays a critical role in photocatalytic dye removal. The visible yellow light with powers 50 and 10 watt respectively were applied. Fig. (4-13) shows the degradation efficiency at both powers with, it is obvious that the power of 10 W is not sufficient to cause a significant degradation of M.B. due to very low number of emitted photons [37]. See table A6 in appendix.

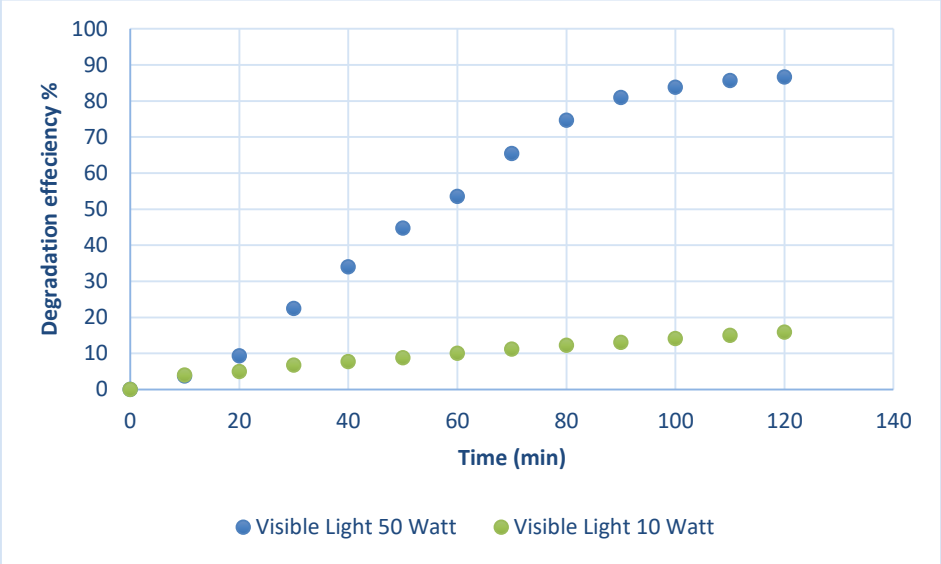

Figure (4-15): Effect of light source on M.B photodegradation performance by CQDs.

4.6 Effect of Initial Concentration of M.B Pollutant

Three concentrations of M.B (35, 23.33, 17.5) µM were spiked with same amounts of CQDs and irradiated for 120 minutes, the degradation efficiency versus time is illustrated in Fig. (4-14). See table A7 in appendix.

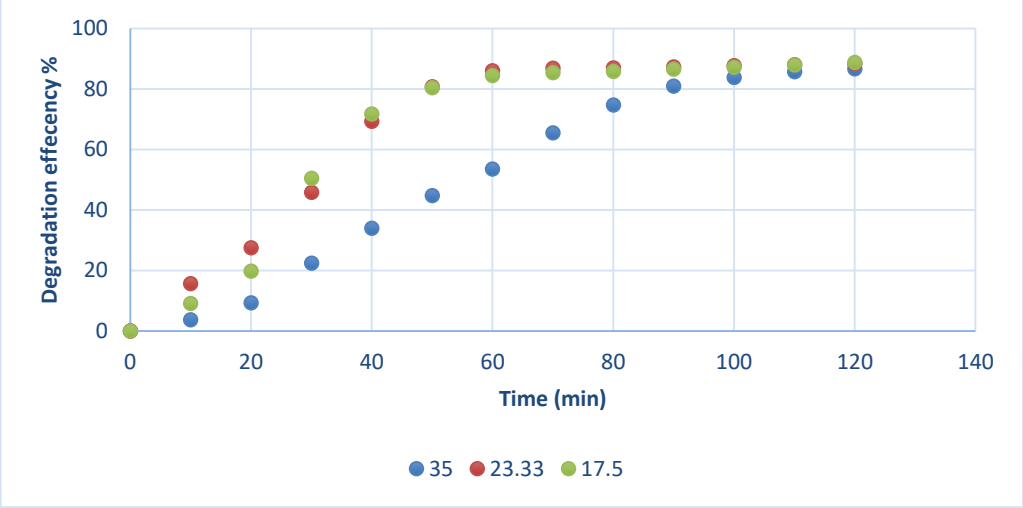

Figure (4-16): Effect of amounts of pollutant (M.B) on M.B photodegradation performance by CQDs under visible yellow light.

The degradation rate as in Fig (4-16). Decreases with the increase of M.B concentration. As photodegradation occurs due to light absorption by CQDs, this decrease could be ascribed to that excessive M.B may hamper the reception of light onto the CQDs surface to activate the photocatalytic processes [38]. See Fig. (4-17).

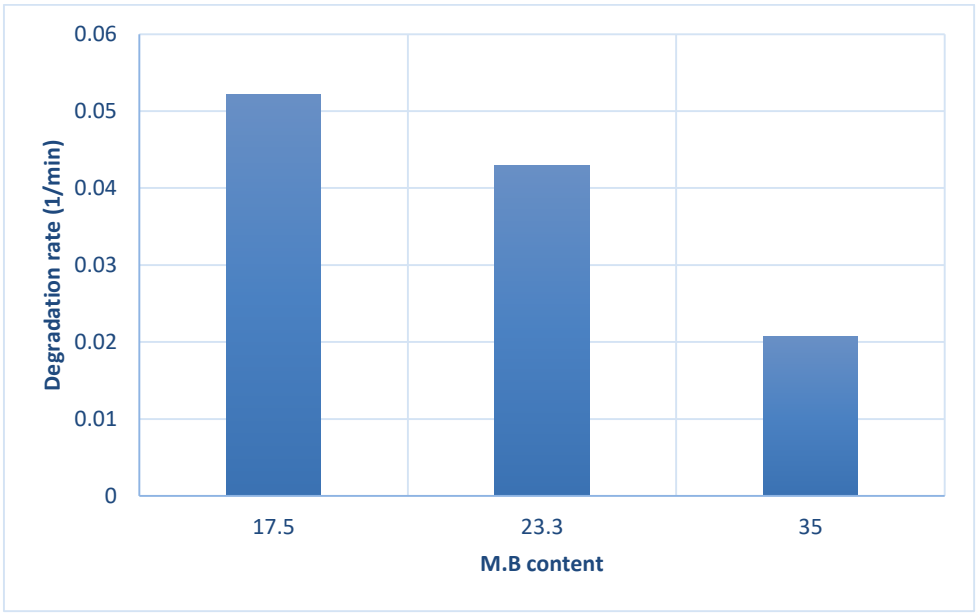

Figure (4-17): Degradation rate at different pH content.

4.7 CQDs\ZnO Nanocomposite

Due to the unique properties of carbon quantum dots and ease of coupling to other materials to get composite, it was able to prepare CQDs\ZnO nanocomposite. The

prepared nanocomposite was tested as a photocatalyst for the degradation of M.B studying the effect of introducing of CQDs onto ZnO surface.

The results were shown in Fig. (4-14) and table A8 in appendix the efficiency of degradation was greater in composite compared with bare ZnO, furthermore the degradation rate of M.B was improved from 0.07 1/min for bare ZnO to about to 0.012 1/min for CQDs/ZnO composite.

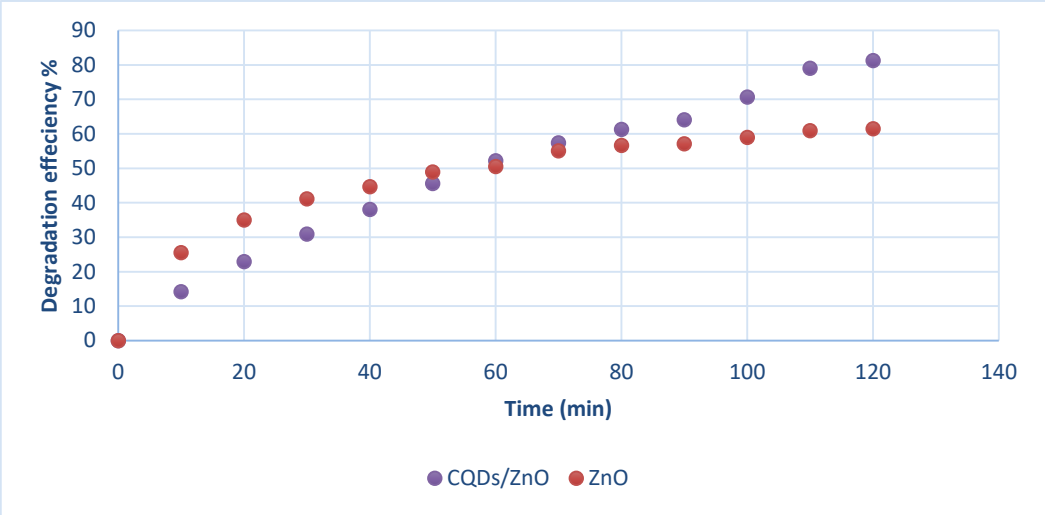

Figure (4-18): comaprision of CQDs/ZnO and ZnO alone on degradation of M.B under visible yellow light.

The enhanced photocatalytic activity of CQDs/ZnO toward the degradation of M.B was explained by the increased effective contact area and the changed surface charge of zinc oxide due to the CQDs as well as large surface area and excellent electron conductivity of the photogenerated carriers. In a CQDs/ZnO-based visible-light system, the superoxide radical (O2 -) and the hole (h+) species were found to participate in the target reactions, providing direct evidence to account for the enhanced photocatalytic activity of CQDs/ ZnO. In addition, CQDs/ZnO exhibited adequate catalytic stability, performing as a genuine visible-light-driven photocatalyst to decompose aqueous organic pollutants effectively [39].

In brief, the superior ability of CQDs/ZnO to capture and transfer electrons enhanced the efficiency of the separation of photogenerated electron–hole pairs so that it could be adequately related to the photocatalytic process, and a richly efficient photocatalytic activity could be attained [27].

Chapter Five: Conclusion

An efficient visible-light photocatalyst CQDs was facilely prepared by top-down route using pyrolysis chemical oxidation method. The photocatalytic activity of the as-prepared CQDs was evaluated by monitoring the degradation of methylene blue (M.B) under visible yellow light irradiation (50 W) within 120 min. For all photocatalysis experiments, aqueous M.B solution with an initial concentration of 35 μM was used.

In addition, dose of CQDs promoted the degradation of M.B due to increase in catalyst sites. Increase the pH have the highest percentage of absorption and the speed of degradation among of the other factors, where at pH 10.6 the degradation rate was 0.02026, while the degradation efficiency was 92%. It was also found that increasing sodium chloride salt (NaCl) content leads to a decrease in the rate of degradation. Also, due to quantity of photons, light source and location affected the degradation rate and efficiency, where more degradation was occurred at close distance. Pollutant contents were tested, where excessive M.B hampered the reception of light needed to activate the photocatalytic processes.

It also turns out that a composite can be made with carbon quantum dots by mixing it with other photocatalysts as ZnO to increase of degradation rate and this allows the electrode to be manufactured.

Chapter Six: References

1. Xu, X., et al., *Electrophoretic Analysis and Purification of Fluorescent Single-Walled Carbon Nanotube Fragments.* Journal of the American Chemical Society, 2004. **126**(40): p. 12736-12737.
2. Cheng, Y., et al., *Synthesis of fluorescent carbon quantum dots from aqua mesophase pitch and their photocatalytic degradation activity of organic dyes.* Journal of Materials Science & Technology, 2019. **35**(8): p. 1515-1522.
3. Yadav, A., et al., *Lasing behavior of surface functionalized carbon quantum dot/RhB composites.* Nanoscale, 2017. **9**(16): p. 5049-5054.
4. Das, R., R. Bandyopadhyay, and P. Pramanik, *Carbon quantum dots from natural resource: A review*. Materials Today Chemistry, 2018. **8**: p. 96-109.
5. Namdari, P., B. Negahdari, and A. Eatemadi, *Synthesis, properties and biomedical applications of carbon-based quantum dots: An updated review.* Biomedicine & Pharmacotherapy, 2017. **87**: p. 209-222.
6. Di, J., et al., *Novel visible-light-driven CQDs/Bi2WO6 hybrid materials with enhanced photocatalytic activity toward organic pollutants degradation and mechanism insight.* Applied Catalysis B: Environmental, 2015. **168-169**: p. 51-61.
7. Zhang, X., et al., *Natural-Product-Derived Carbon Dots: From Natural Products to Functional Materials.* ChemSusChem, 2018. **11**(1): p. 11-24.
8. Miao, P., et al., *Recent advances in carbon nanodots: synthesis, properties and biomedical applications.* Nanoscale, 2015. **7**(5): p. 1586-1595.
9. Dey, S., et al., *Luminescence properties of boron and nitrogen doped graphene quantum dots prepared from arc-discharge-generated doped graphene samples.* Chemical Physics Letters, 2014. **595-596**: p. 203-208.
10. Cao, L., et al., *Carbon Dots for Multiphoton Bioimaging.* Journal of the American Chemical Society, 2007. **129**(37): p. 11318-11319.
11. Wang, R., et al., *Recent progress in carbon quantum dots: synthesis, properties and applications in photocatalysis.* Journal of Materials Chemistry A, 2017. **5**(8): p. 3717-3734.
12. Li, H., et al., *Carbon nanodots: synthesis, properties and applications.* Journal of Materials Chemistry, 2012. **22**(46): p. 24230-24253.

13. Sahu, S., et al., *Simple one-step synthesis of highly luminescent carbon dots from orange juice: application as excellent bio-imaging agents.* Chemical Communications, 2012. **48**(70): p. 8835-8837.
14. Gao, X., et al., *A composite material of vacuum heat-treated CQDs/Ce0.7Zr0.3O2 with enhanced charge separation for efficient photocatalytic degradation.* Vacuum, 2019. **169**: p. 108912.
15. Gong, N., et al., *Microwave-Assisted Polyol Synthesis of Gadolinium-Doped Green Luminescent Carbon Dots as a Bimodal Nanoprobe.* Langmuir, 2014. **30**(36): p. 10933-10939.
16. Liu, X.-P., J. Yang, and Y. Bai, *Determination of ferric ions based on fluorescence quenching of carbon dots.* Chinese Journal of Analytical Chemistry, 2016. **44**(5): p. 804-808.
17. Sciortino, A., A. Cannizzo, and F. Messina, *Carbon nanodots: a review—from the current understanding of the fundamental photophysics to the full control of the optical response.* C—Journal of Carbon Research, 2018. **4**(4): p. 67.
18. Desa, A.L., et al., *Industrial textile wastewater treatment via membrane photocatalytic reactor (MPR) in the presence of ZnO-PEG nanoparticles and tight ultrafiltration.* Journal of Water Process Engineering, 2019. **31**: p. 100872.
19. Ong, C.B., A.W. Mohammad, and L.Y. Ng, *Integrated adsorption-solar photocatalytic membrane reactor for degradation of hazardous Congo red using Fe-doped ZnO and Fe-doped ZnO/rGO nanocomposites.* Environmental Science and Pollution Research, 2019. **26**(33): p. 33856-33869.
20. Rani, U.A., et al., *Sustainable production of nitrogen-doped carbon quantum dots for photocatalytic degradation of methylene blue and malachite green.* Journal of Water Process Engineering, 2021. **40**: p. 101816.
21. Abdulla, N.K., et al., *Psidium guajava leave-based magnetic nanocomposite γ-Fe2O3@GL: A green technology for methylene blue removal from water.* Journal of Environmental Chemical Engineering, 2019. **7**(6): p. 103423.
22. Üner, O., *Hydrogen storage capacity and methylene blue adsorption performance of activated carbon produced from Arundo donax.* Materials Chemistry and Physics, 2019. **237**: p. 121858.
23. Rani, U.A., et al., *A review of carbon quantum dots and their applications in wastewater treatment.* Advances in Colloid and Interface Science, 2020. **278**: p. 102124.

24. Zhou, C., et al., *Distorted polymeric carbon nitride via carriers transfer bridges with superior photocatalytic activity for organic pollutants oxidation and hydrogen production under visible light.* Journal of Hazardous Materials, 2020. **386**: p. 121947.
25. Wang, F., et al., *Construction of novel Z-scheme nitrogen-doped carbon dots/{0 0 1} TiO2 nanosheet photocatalysts for broad-spectrum-driven diclofenac degradation: Mechanism insight, products and effects of natural water matrices.* Chemical Engineering Journal, 2019. **356**: p. 857-868.
26. Yu, H., et al., *Enhanced photocatalytic tetracycline degradation using N-CQDs/OV-BiOBr composites: Unraveling the complementary effects between N-CQDs and oxygen vacancy.* Chemical Engineering Journal, 2020. **402**: p. 126187.
27. Lu, Q., Y. Zhang, and S. Liu, *Graphene quantum dots enhanced photocatalytic activity of zinc porphyrin toward the degradation of methylene blue under visible-light irradiation.* Journal of Materials Chemistry A, 2015. **3**(16): p. 8552-8558.
28. Jiang, R., et al., *Insights into a CQD-SnNb2O6/BiOCl Z-scheme system for the degradation of benzocaine: Influence factors, intermediate toxicity and photocatalytic mechanism.* Chemical Engineering Journal, 2019. **374**: p. 79-90.
29. Singh, A., et al., *Pollutant Soot for Pollutant Dye Degradation: Soluble Graphene Nanosheets for Visible Light Induced Photodegradation of Methylene Blue.* ACS Sustainable Chemistry & Engineering, 2017. **5**(10): p. 8860-8869.
30. Carneiro, J.O., et al., *13 - Self-cleaning smart nanocoatings*, in *Nanocoatings and Ultra-Thin Films*, A.S.H. Makhlouf and I. Tiginyanu, Editors. 2011, Woodhead Publishing. p. 397-413.
31. Peng, Z., et al., *Facile synthesis of "boron-doped" carbon dots and their application in visible-light-driven photocatalytic degradation of organic dyes.* Nanomaterials, 2020. **10**(8): p. 1560.
32. Sawalha, S., et al., *Tailoring the sensing abilities of carbon nanodots obtained from olive solid wastes.* Carbon, 2020. **167**: p. 696-708.
33. Das, G.S., et al., *Biomass-derived carbon quantum dots for visible-light-induced photocatalysis and label-free detection of Fe (III) and ascorbic acid.* Scientific reports, 2019. **9**(1): p. 1-9.

34. Zhou, Y., et al., *Size-dependent photocatalytic activity of carbon dots with surface-state determined photoluminescence.* Applied Catalysis B: Environmental, 2019. **248**: p. 157-166.
35. Hu, S., et al., *Modulation and effects of surface groups on photoluminescence and photocatalytic activity of carbon dots.* Nanoscale, 2013. **5**(23): p. 11665-11671.
36. Lin, X., et al., *Graphitic carbon nitride quantum dots and nitrogen-doped carbon quantum dots co-decorated with BiVO4 microspheres: A ternary heterostructure photocatalyst for water purification.* Separation and Purification Technology, 2019. **226**: p. 117-127.
37. Anwer, H., et al., *Photocatalysts for degradation of dyes in industrial effluents: Opportunities and challenges.* Nano Research, 2019. **12**(5): p. 955-972.
38. Chen, J., et al., *Synthesis of carbon quantum dots/TiO2 nanocomposite for photo-degradation of Rhodamine B and cefradine.* Diamond and Related Materials, 2016. **70**: p. 137-144.
39. Zhang, J., et al., *Enhanced antibacterial properties of the bracket under natural light via decoration with ZnO/carbon quantum dots composite coating.* Chemical Physics Letters, 2018. **706**: p. 702-707.
40. Kumar, D., et al., *Synthesis and Characterization of Carbon Quantum Dots from Orange Juice.* Journal of Bionanoscience, 2014. **8**: p. 274-279.
41. Thakur, A., et al., *TiO2 nanofibres decorated with green-synthesized PAu/Ag@CQDs for the efficient photocatalytic degradation of organic dyes and pharmaceutical drugs.* RSC Advances, 2020. **10**(15): p. 8941-8948.
42. Di, J., et al., *Novel visible-light-driven CQDs/Bi2WO6 hybrid materials with enhanced photocatalytic activity toward organic pollutants degradation and mechanism insight.* Applied Catalysis B-environmental, 2015. **168**: p. 51-61.
43. Pan, J., et al., *Structure of Z-scheme CdS/CQDs/BiOCl heterojunction with enhanced photocatalytic activity for environmental pollutant elimination.* Applied Surface Science, 2018. **444**: p. 177.
44. Kaur, S., S. Sharma, and S. Kansal, *Synthesis of ZnS/CQDs nanocomposite and its application as a photocatalyst for the degradation of an anionic dye, ARS.* Superlattices and Microstructures, 2016. **98**.

45. Sang, L., J. Lin, and Y. Zhao, *Preparation of carbon dots/TiO2 electrodes and their photoelectrochemical activities for water splitting.* International Journal of Hydrogen Energy, 2017. **42**(17): p. 12122-12132.
46. Gopal, A., D. Jose, and Sivagnanam, *Fabrication of ZnO/ZnO at carbon dot as photo anode and Natural dye as photosensitizer for dye sensitized solar cell application.* International Journal of Engineering and Technology(UAE), 2018. **7**: p. 107-110.
47. Sun, M., et al., *A nanocomposite of carbon quantum dots and TiO2 nanotube arrays: enhancing photoelectrochemical and photocatalytic properties.* RSC Advances, 2014. **4**(3): p. 1120-1127.
48. Wang, F., et al., *Construction of novel Z-scheme nitrogen-doped carbon dots/{001} TiO2 nanosheet photocatalysts for broad-spectrum-driven diclofenac degradation: Mechanism insight, products and effects of natural water matrices.* Chemical Engineering Journal, 2018. **356**.
49. Jiang, W., et al., *Enhanced visible-light-induced photocatalytic degradation of tetracycline using BiOI/MIL-125(Ti) composite photocatalyst.* Journal of Alloys and Compounds, 2021. **854**: p. 157166.
50. Zhang, Z., et al., *Enhanced Photocatalytic Activity toward Organic Pollutants Degradation and Mechanism Insight of Novel CQDs/Bi2O2CO3 Composite.* Nanomaterials, 2018. **8**(5): p. 330.
51. Luo, L., et al., *Facile fabrication of metal-free urchin-like g-C3N4 with superior photocatalytic activity.* RSC Advances, 2016. **6**(97): p. 94496-94501.
52. Tai, J.Y., et al., *Facile green synthesis of fingernails derived carbon quantum dots for Cu2+ sensing and photodegradation of 2,4-dichlorophenol.* Journal of Environmental Chemical Engineering, 2020: p. 104622.
53. Zhao, J., et al., *Fabrication of CQDs/Bi5Nb3O15 nanocomposites for photocatalytic degradation of veterinary pharmaceutical sarafloxacin.* Catalysis Today, 2020. **355**: p. 716-726.
54. Kim, M.G. and W.-K. Jo, *Visible-light-activated N-doped CQDs/g-C3N4/Bi2WO6 nanocomposites with different component arrangements for the promoted degradation of hazardous vapors.* Journal of Materials Science & Technology, 2020. **40**: p. 168-175.

55. Chen, Q., et al., *Photocatalytic degradation of amoxicillin by carbon quantum dots modified K2Ti6O13 nanotubes: Effect of light wavelength.* Chinese Chemical Letters, 2019. **30**(6): p. 1214-1218.
56. Wang, F., et al., *Novel ternary photocatalyst of single atom-dispersed silver and carbon quantum dots co-loaded with ultrathin g-C3N4 for broad spectrum photocatalytic degradation of naproxen.* Applied Catalysis B: Environmental, 2018. **221**: p. 510-520.
57. Liu, W., et al., *Visible-light-driven photocatalytic degradation of diclofenac by carbon quantum dots modified porous g-C3N4: Mechanisms, degradation pathway and DFT calculation.* Water Research, 2019. **151**: p. 8-19.
58. Yu, X., et al., *Preparation and visible light photocatalytic activity of carbon quantum dots/TiO2 nanosheet composites.* Carbon, 2014. **68**: p. 718-724.
59. Guo, Y., F. Cao, and Y. Li, *Solid phase synthesis of nitrogen and phosphor co-doped carbon quantum dots for sensing Fe3+ and the enhanced photocatalytic degradation of dyes.* Sensors and Actuators B: Chemical, 2018. **255**: p. 1105-1111.
60. Mohammad, N.N., K.M. Omer, and S. Baban, *Valorization of tire wastes to carbon quantum dots (P-CDs) and photocatalytic degradation enhancement of organic wastes using ZnO-CDs nanocomposites.* Journal of Materials Science: Materials in Electronics, 2019. **30**(12): p. 11598-11606.
61. Hu, Z., et al., *Rational construct CQDs/BiOCOOH/uCN photocatalyst with excellent photocatalytic performance for degradation of sulfathiazole.* Chemical Engineering Journal, 2021. **404**: p. 126541.
62. Chen, B., et al., *CQDs/Au NPs modified polysulfone membrane with antibacterial function and photocatalytic activity for degradation of methylene blue.* Nano, 2020.
63. Liu, Y., et al., *In situ assembly of CQDs/Bi2WO6 for highly efficient photocatalytic degradation of VOCs under visible light.* New Journal of Chemistry, 2020. **44**(8): p. 3455-3462.
64. Das, G.S., et al., *Biomass-derived Carbon Quantum Dots for Visible-Light-Induced Photocatalysis and Label-Free Detection of Fe(III) and Ascorbic acid.* Scientific Reports, 2019. **9**(1): p. 15084.

65. Hak, C., et al., *Water hyacinth derived carbon quantum dots and g-C3N4 composites for sunlight driven photodegradation of 2,4-dichlorophenol.* SN Applied Sciences, 2020. **2**.
66. Chen, Y., et al., *Enhanced Photocatalytic Activity of the Carbon Quantum Dot-Modified BiOI Microsphere.* Nanoscale Research Letters, 2016. **11**(1): p. 60.
67. Hu, Y., et al., *Visible-Light Upconversion Carbon Quantum Dots Decorated TiO₂ for the Photodegradation of Flowing Gaseous Acetaldehyde.* Applied Surface Science, 2018. **440**: p. 266.
68. Mahmood, A., et al., *Carbon quantum dots-TiO2 nanocomposite as an efficient photocatalyst for the photodegradation of aromatic ring-containing mixed VOCs: An experimental and DFT studies of adsorption and electronic structure of the interface.* Journal of Hazardous Materials, 2021. **401**: p. 123402.
69. Zhang, J., et al., *Coal tar pitch as natural carbon quantum dots decorated on TiO2 for visible light photodegradation of rhodamine B.* Carbon, 2019. **152**: p. 284-294.
70. Zheng, F., et al., *Synthesis of carbon quantum dot-surface modified P25 nanocomposites for photocatalytic degradation of p-nitrophenol and acid violet 43.* RSC Advances, 2014. **4**(58): p. 30605-30609.
71. Hasija, V., et al., *Carbon quantum dots supported AgI /ZnO/phosphorus doped graphitic carbon nitride as Z-scheme photocatalyst for efficient photodegradation of 2, 4-dinitrophenol.* Journal of Environmental Chemical Engineering, 2019. **7**(4): p. 103272.
72. Hu, Y., et al., *Visible-Light Upconversion Carbon Quantum Dots Decorated TiO2 for the Photodegradation of Flowing Gaseous Acetaldehyde.* Applied Surface Science, 2018. **440**: p. 266-274.
73. Wang, Y., et al., *Facile synthesis of carbon quantum dots loaded with mesoporous g-C3N4 for synergistic absorption and visible light photodegradation of fluoroquinolone antibiotics.* Dalton Transactions, 2018. **47**(4): p. 1284-1293.
74. Aji, M., et al., *Carbon Nanodots from Frying Oil as Catalyst for Photocatalytic Degradation of Methylene Blue Assisted Solar Light Irradiation.* American Journal of Applied Sciences, 2016. **13**: p. 432-438.
75. Meng, F., et al., *Synthesis of CQDs@FeOOH nanoneedles with abundant active edges for efficient electro-catalytic degradation of levofloxacin: Degradation*

mechanism and toxicity assessment. Applied Catalysis B: Environmental, 2021. **282**: p. 119597.

76. Chen, P., et al., *Accelerated photocatalytic degradation of diclofenac by a novel CQDs/BiOCOOH hybrid material under visible-light irradiation: Dechloridation, detoxicity, and a new superoxide radical model study.* Chemical Engineering Journal, 2018. **332**: p. 737-748.
77. Kaur, S., S. Sharma, and S.K. Kansal, *Synthesis of ZnS/CQDs nanocomposite and its application as a photocatalyst for the degradation of an anionic dye, ARS.* Superlattices and Microstructures, 2016. **98**: p. 86-95.
78. Das, R., J. Kar, and S. Mohapatra, *Enhanced Photodegradation of Organic Pollutants by Carbon Quantum Dot (CQD) Deposited Fe3O4@m-TiO2 Nano Kooshballs.* Industrial & Engineering Chemistry Research, 2016. **55**.
79. Wu, Q., et al., *Effect of reaction temperature on properties of carbon nanodots and their visible-light photocatalytic degradation of tetracyline.* RSC Advances, 2015. **5**(92): p. 75711-75721.
80. Guo, Y., et al., *A novel method for the development of a carbon quantum dot/carbon nitride hybrid photocatalyst that responds to infrared light irradiation.* Journal of Materials Chemistry A, 2015. **3**(25): p. 13189-13192.
81. Omer, K.M., et al., *Carbon nanodots as efficient photosensitizers to enhance visible-light driven photocatalytic activity.* Journal of Photochemistry and Photobiology A: Chemistry, 2018. **364**: p. 53-58.
82. Sun, A.-C., *Synthesis of magnetic carbon nanodots for recyclable photocatalytic degradation of organic compounds in visible light.* Advanced Powder Technology, 2018. **29**(3): p. 719-725.
83. Gao, X., et al., *Carbon quantum dots promote charge transfer of Ce0.7Zr0.3O2@Bi2MoO6 heterojunction for efficient photodegradation of RhB in visible region.* Optical Materials, 2020. **105**: p. 109828.
84. Di, J., et al., *The synergistic role of carbon quantum dots for the improved photocatalytic performance of Bi2MoO6.* Nanoscale, 2015. **7**(26): p. 11433-11443.
85. Koe, W.S., et al., *Novel nitrogen and sulphur co-doped carbon quantum dots/titanium oxide photocatalytic membrane for in-situ degradation and removal of pharmaceutical compound.* Journal of Water Process Engineering, 2020. **33**: p. 101068.

86. Saud, P.S., et al., *Carbon quantum dots anchored TiO2 nanofibers: Effective photocatalyst for waste water treatment.* Ceramics International, 2015. **41**(9, Part B): p. 11953-11959.
87. Xia, J., et al., *Ionic liquid-induced strategy for carbon quantum dots/BiOX (X=Br, Cl) hybrid nanosheets with superior visible light-driven photocatalysis.* Applied Catalysis B: Environmental, 2016. **181**: p. 260-269.
88. Gao, H., et al., *Construction of a CQDs/Ag3PO4/BiPO4 Heterostructure Photocatalyst with Enhanced Photocatalytic Degradation of Rhodamine B under Simulated Solar Irradiation.* Micromachines, 2019. **10**(9): p. 557.
89. Yu, H., et al., *ZnO/carbon quantum dots nanocomposites: One-step fabrication and superior photocatalytic ability for toxic gas degradation under visible light at room temperature.* New J. Chem., 2012. **36**: p. 1031-1035.
90. Liang, M., et al., *Design of a Z-scheme g-C3N4/CQDs/CdIn2S4 composite for efficient visible-light-driven photocatalytic degradation of ibuprofen.* Environmental Pollution, 2020. **259**: p. 113770.
91. Liang, H., X. Tai, and Z. Du, *Photocatalytic degradation of nonylphenol ethoxylate and its degradation mechanism.* Journal of Molecular Liquids, 2020. **302**: p. 112567.
92. Xian, T., et al., *Carbon Quantum Dots (CQDs) Decorated Bi2O3-x Hybrid Photocatalysts with Promising NIR-Light-Driven Photodegradation Activity for AO7.* Catalysts, 2019. **9**(12): p. 1031.
93. Duo, F., et al., *Enhanced visible light photocatalytic activity and stability of CQDs/BiOBr composites: The upconversion effect of CQDs.* Journal of Alloys and Compounds, 2016. **685**: p. 34-41.
94. Sharma, S., et al., *Promising photocatalytic degradation of lignin over carbon quantum dots decorated TiO2 nanocomposite in aqueous condition.* Applied Catalysis A: General, 2020. **602**: p. 117730.
95. Aji, M.P., et al., *Carbon nanodots from frying oil as catalyst for photocatalytic degradation of methylene blue assisted solar light irradiation.* Am. J. Appl. Sci, 2016. **13**(4): p. 432-438.
96. Zhang, Y.-Q., et al., *N-doped carbon quantum dots for TiO2-based photocatalysts and dye-sensitized solar cells.* Nano Energy, 2013. **2**(5): p. 545-552.

97. Umrao, S., et al., *Multi-layered graphene quantum dots derived photodegradation mechanism of methylene blue.* RSC Advances, 2015. **5**(64): p. 51790-51798.
98. Ma, Z., et al., *One-step ultrasonic synthesis of fluorescent N-doped carbon dots from glucose and their visible-light sensitive photocatalytic ability.* New Journal of Chemistry, 2012. **36**(4): p. 861-864.

Chapter Seven: Appendix

Table A 1: Applications of CQDs as photocatalysis (comprehensive review).

#	Sources	Size (nm)	Application	CQDs / Additions	The role of the CQDs in the application	How CQDs made	References
	Orange juice	3.8	Photosensitizer in water splitting	With TiO_2	Strong and stable photoluminescence	Hydrothermal method	[40]
2	Citrus limetta waste	4-7	Degradation of organic dyes	With Au and Ag	Sole reducing and capping agent	By the continuous stirring of the HAuCl4 and CQD solution	[41]
3	Graphite particles	6	Organic pollutants degradation	With Bi_2WO_6	Photocatalytic activities of Bi2WO6 on RhB, CIP, BPA and TC (pollutants) degradation under visible light irradiation increased dramatically	Hydrothermal method	[42]
4	Glucose sugar		Photocatalytic activity for environmental pollutant	With CdS and BiOCl	The photocatalytic performance tests reveal that the CdS/CQDs/BiOCl heterojunction exhibits much higher photocatalytic activity than that of BiOCl, CdS/BiOCl	Synthesized by a stepwise facile region-selective (deposition process)	[43]

		2-5	elimination (phenol contaminant)				
5	Graphene oxide	5	Degradation of an anionic dye, ARS	With ZnS	The results showed that the ZnS/CQDs exhibited excellent photocatalytic activity for the degradation of ARS dye i.e., 89% higher than that of the bare ZnS (63%).	Via a fast and facile chemical precipitation technique	[44]
6	Graphite	4.12 ± 0.97	Water splitting	With TiO_2 electrodes	-Serve as sensitizer TiO_2 photoelectrode in water splitting system of alkaline solution.	Electrochemical ablation	[45]
7	Neem leaves	<10	Dye sensitized solar cell application	With ZnO	Enhances the power conversion efficiencies of DSSC.	Hydrothermal treatment	[46]
8	Graphite electrodes.	<4	Enhancing photoelectrochemical and photocatalytic properties	With TiO_2 nanotube arrays	Improving the utilization of visible light for TiO_2 nanotube arrays.	Electrochemical-etching	[47]
9	Citric acid, urea	<10	photocatalytic degradation of diclofenac	With BiOCOOH	CQDs increased the light absorption and charge transfer and separation of BiOCOOH.	Hydrothermal treatment	[48]

10	Aqueous solution of glucose and HCl	50	photocatalytic activity for the degradation of tetracycline	With MIL-125(Ti)	The efficiency of degradation could reach 80%, which is much higher than that of bare BiOI and MIL-125(Ti).	Hydrothermal treatment	[49]
11	Graphite rods	2-5	Photocatalytic toward Organic Pollutants Degradation	With Bi_2O2CO_3	CQDs/$Bi_2O_2CO_3$ possess an efficient photocatalytic performance, and the organic matter removal rate of methylene blue and phenol can reach up to 94.45% and 61.46% respectively	Hydrothermal treatment	[50]
12	Citric acid and ethylene diamine	5	Photocatalysts for RhB and TC-HCl degradation	With g-C_3N_4	The reaction rate constant for the photodegradation of RhB and TC-HCl were about increased 3.7-fold and 1.9-fold higher than that of bare g-C3N4	By a facile low temperature method.	[51]
13	Sgrinded fingernail silica as a green precursor	1.72-5.85	Photodegradation of 2,4-dichlorophenol	With g-C_3N_4	Act as photosensitizer to increase the light absorption range to generate more electron and holes	Hydrothermal treatment	[52]
14	Citric acid urea	10	Photocatalytic degradation of veterinary pharmaceutical sarafloxacin	With $Bi_5Nb_3O_{15}$	Nanocomposites exhibited better degradation efficiency than pure Bi5Nb3O15 nanoparticles	Hydrothermal method	[53]

15	Citric acid and ethanediamine	2.5-9.4	Degradation of hazardous vapors	With g-C_3N_4/Bi_2WO_6	A favorable long-term photocatalyst for environmental decontamination (Photochemical stability) and revealed higher removal efficiencies	Hydrothermal method	[54]
16	HCl solution	6	Photocatalytic degradation of amoxicillin	With $K_2Ti_6O_{13}$	Promoting photocatalytic activity	Hydrothermal treatment combined with calcinations	[55]
17	Citric acid and ethanediamine	4	Photocatalytic degradation of naproxen	With g-C_3N_4/ SDAg	Gives 10-fold higher reaction rate	Thermo-polymerization method	[56]
18	Citric acid and of urea	<10	Degradation diclofenac	With g-C_3N_4	Gives 15 times success higher reaction rate. . The presence of CQDs broadens the absorption spectrum of g-C3N4 and act as charge carriers for photo-generated electrons (e-), resulting in enhanced photocatalytic activity of CNCs.	Hydrothermal	[57]

19	Ethanol	5	Degradation of rhodamine B	With TiO_2 /TNS composites.	The degradation efficiency increases gradually from 27.2% to 95.4%, which indicates that introducing a suitable amount of C QDs can effectively improve the visible photocatalytic activity of TNS for the degradation of RhB	Hydrothermal method	[58]
20	Mixture of citric acid and O-phosphory lethanol amine.	3.03 ±1.01	Degradation of dyes under sunlight irradiation	With TiO_2 and phosphor	Can greatly enhance the photocatalytic activity of TiO2 nanoparticles for photocatalytic degradation of dyes.	Thermal treatment	[59]
21	Aqua mesophase pitch (AMP)	2.8	Degrading rhodamine B (Rh B), methyl blue (M.B) and indigo carmine (IC) (organic fyes).	Alone	CQDs can increase the surface traps of absorbtion band.	Hydrothermal method	[2]
22	Solid tire wastes	2-3	photodegrade an organic compound such as methylene blue	Zno P	increase visible light response due to carbon edge absorption	Hydrothermal method	[60]

23	Citrate acid and ethylene diamine	2 – 10	Degradation of sulfathiazole	With BiOCOOH and uCN	Where carbon quantum dots (CQDs) acted as mediators to shuttle electrons between BiOCOOH and ultrathin g-C3N4 nanosheets (uCN), to modulate the migration route of photogenerated carriers.	Hydrothermal method	[61]
24	polyethyleneimine-10000 (PEI)	<10	Degradation of methylene blue	With Au NPs	Improve the antibacterial property of the membrane	Hydrothermal synthesis	[62]
25	Different carbonaceous materials	3-5	Degradation of VOCs under Visible Light	With Bi_2WO_6	Performed excellent activity in the photocatalytic degradation of VOCs under visible light irradiation	Synthesized by a hydrothermal method	[63]
26	Carbonized starch	20	Photo-degradation of Rhodamine B and cefradine	With TiO_2	Ability to extend the visible absorption and produce more electrons and electron–hole pairs for the degradation of pollutants**.**	Chemical oxidation	[38]
27	Pear juice	10	Visible-Light-Induced Photocatalysis	Alone	Visible light-responsive photocatalyst for the efcient degradation of methylene blue (M.B) as a model pollutant dye.	By a facile hydrothermal process.	[64]

28	Water hyacinth leaves	3.1	Sunlight driven photodegradation of 2,4-dichlorophenol	g-C_3N4 composites	Elongating the lifetime of photogenerated electrons and widening the visible light response.	Hydrothermal treatment	[65]
29	Bismuth oxyhalides	2	Enhanced Photocatalytic Activity of the CQDs	BiOL	Increase the photocatalytic activities of degradation of MO under visible light irradiation greatly.	Facile hydrothermal treatment process	[66]
30	Gaseous pollutant	4 ~ 5	Photodegradation of Flowing Gaseous Acetaldehyde	TiO_2	Obtain the highest photodegradation efficiency by constructed the CQDs/TiO2 heterostructured photocatalyst under visible-light irradiation.	Hydrothermal method	[67]
31	Citric acid	2.4	Photodegradation of aromatic ring-containing mixed VOCs	TiO_2	To optimum better photocatalytic performance	Hydrothermal method and citrate precursor method	[68]
32	Coal tar pitch	5.17 ± 0.95	Visible light photodegradation of rhodamine B	TiO_2	Use of CTP as a natural alternative for CQDs, and prepare effective CTP/TiO2 composite photocatalysts by a simple green by a simple green one step solvothermal method.	By a simple and environmentally friendly one-step solvothermal method	[69]
33	Ethanol, NaOH	2-10	Photocatalytic degradation of p-	Modified P_{25} nanocomposites	Preparing a new efficient and stable visible light driven photocatalyst	Electrolytic denudation method	[70]

	and graphite		nitrophenol and acid violet 43				
34	Bamboo leaves	< 10	Z-scheme photocatalyst for efficient photodegradation of 2, 4-dinitrophenol	AgI /ZnO/phosphorus doped graphitic carbon nitride	Offers a green and facile route for visible light driven and stable nonmetal doped photocatalyst	Hydrothermal method	[71]
35	Citric acid and urea	4 ~ 5	Photodegradation of Flowing Gaseous Acetaldehyde	TiO_2	To enhance the photocatalytic performance of TiO2-based composites for flowing gaseous acetaldehyde removal	Hydrothermal method	[72]
36	Citric acid	2-10	Synergistic absorption and visible light photodegradation of fluoroquinolone antibiotics	Mesoporous g-C_3N_4	Enhance the capacity for the adsorption of fluoroquinolones antibiotics (FQs)	Simple hydrothermal method	[73]
37	Frying Oil	<10	Photocatalyticdegradation of methylene blue solution with assisted solar lightirradiatin.	Only	Catalyst in the photocatalytic process of methylene blue solution.	Hydrothermal treatment	[74]

38	Orange peel	<10	Degradation of levofloxacin	FeOOH	-The structure modifier - mainly attributed to the high % OH generation ability and high mass transfer ability of the needles.	Hydrothermal oxidation	[75]
39	$ZnIn_2S_4$/ BiOCl van der Waals (VDW)	3	Degradation of benzocaine	$SnNb_2O_6$/BiOCl Z-scheme system	Bridge for the charge carriers	Facile hydrothermal method	[28]
40	$ZnIn_2S_4$/ BiOCl van der Waals (VDW)	2 – 10	Degradation of diclofenac	BiOCOOH	Modify BiOCOOH with the aim of negating the UV limit of the photocatalyst, while increasing its photocatalytic activity.	Hydrothermal process	[76]
41	Ascorbic acid	<10	Degradation of an anionic dye, ARS	ZnS	A photocatalyst for the degradation of Alizarin red S (ARS) dye under visible light irradiation.	Fast and facile chemical precipitation technique	[77]
42	Ammonium citrate	<10	Degradation of tetracycline	OV-BiOBr	Regulated the single-electron reduction of dissolved oxygen to produce superoxide radicals (%O2 −) and OV mainly drove the robust H2O2 generation via two-electron reduction of the chemisorbed oxygen molecules.	Hydrothermal method	[26]

43	Glucose solution	3.86	Degradation of organic pollutants	m TiO_2	Expands the light absorption of mTiO2 from UV to visible region.	Hydrothermal treatment	[78]
44	Larch	~6.48	Degradation of tetracyline	TiO_2	Photogenerated holes could either recombine with electrons, react with OH− or H2O, oxidizing them to highly oxidizing species such as OH• and O2•radicals, or oxidize the adsorbed TCH molecules	Hydrothermal process	[79]
45	Glucose +NaOH	5	Degrade methyl orange	Nitride	CQD acts as the light source to upconvert infrared light to visible light	Hydrothermal process	[80]
46	Uric acid, Hcl and glucose	2-5	Degradation of an environmental organic pollutant	ZnO	Photosensitizer to the wide band gap ZnO nanoparticles lead to high efficiency degradation	Hydrothermal process	[81]
47	Glucose +Sodium hydroxid+acetic acid	5-10	Degradation of organic compounds, Methylene blue	Fe_3O_4	Excite electrons to produce e/h+ pairs under visible light irradiation	Chemical precipitation technique	[82]
48	Larch wood	10	Photodegradation of the Rhodamine B dye under	$Ce_{0.7}Zr_{0.3}O_2$@ Bi_2MoO_2	Act as cocatalysts to further promote efficient charge separation and transfer in such structure	Hydrothermal method	[83]

			visible-light irradiation				
49	Fluorescent carbon-based materials	7	Photodegradation of four different kinds of pollutants, such as ciprofloxacin (CIP), bisphenol A (BPA), tetracycline hydrochloride (TC), and methylene blue (M.B) under visible light irradiation	Bi_2MoO_6	Acted as photocenter for absorbing solar light, charge separation center for suppressing charge recomb ination, and catalytic center for pollutant photo-degradation	Facile hydrothermal process	[84]
50	Nitric acid and sulphuric acid		Photodegradation of pharmaceutical compound namely diclofenac (DCF) in water	TiO_2	Shifted and broadening the light absorption wavelength from UV range to visible light range and enhanced the photodegradation performance	Sessile drop analysis method	[85]
51	Citric acid and urea	3-4	Photodegradation of methylene blue) under visible light irradiation and	TiO_2	Enhanced photocatalytic activity in the degradation of M.B as well as destruction of E. coli as compared to pristine TiO2 nanofiber under the visible light irradiation	Hydrothermal method	[86]

			antibacterial properties				
52	Citric acid	5	Degradation of RhB (phenol rhodamine B), CIP (antibacterial agent ciprofloxacin) and BPA (endocrine disrupting chemical bisphenol A) under visible light irradiation.	BiOBr	Better optical absorption, higher separation efficiency of the photogenerated electron-holes pairs induced by CQDs and smaller resistance	Hydrothermal process	[87]
53	HNO_3 solution	5	Degrading methylene blue	With $Ce_{0.7}Zr_{0.3}O_2$	Enhancing the photocatalytic properties	Hydrothermal method	[14]
54	Graphite	7-10	Photocatalytic Degradation of Rhodamine B	With $Ag_3PO_4/BiPO_4$	Give the synergistic effects of light absorption capacity, thus enhanced photodegradation of the rhodamine B dye	Hydrothermal synthesis method	[88]
55	Solution of cadmium chloride, indium nitrate hydrate	10	Photocatalytic ability for toxic gas degradation (benzene and methanol)	With ZnO	These nanocomposites exhibit higher photocatalytic activity (degradation efficiency over 80%, 24 h) compared to pure ZnO	Electrochemical method	[89]

	and thioacetamide						
56	Graphite	2-3	Photocatalytic degradation of ibuprofen	With g-C_3N_4 /$CdIn2S_4$	Improve photocatalytic performance in the degradation of ibuprofen	Hydrothermal synthesis method	[90]
57	Glucose	6	Photocatalytic degradation of nonylphenol ethoxylate	With TiO_2	Doping can greatly improve the photocatalytic activity and stability of TiO2.	One-step sol-gel method.	[91]
58	Mixing of NaOH-ethanol–H2O-graphite	5	Photodegradation Activity for (acid orange) AO7	With Bi_2O_3	The optimal degradation efficiency of AO7 is achieved 1.38 times higher than the degradation AO7 efficiency pure Bi2O3	Hydrothermal method	[92]
59	L-ascorbic acid and ethanol solution	5	RhB and BPA degradation	With BiOBr	The obtained composites exhibited much higher photocatalytic activity and stability than pure BiOBr under visible light.	Hydrothermal method	[93]
60	Citric acid and	7-9	Photocatalytic degradation of lignin	With TiO_2	Enhanced solar light driven photocatalytic response towards lignin degradation (99 %)	Hydrothermal synthesis	[94]

	ethylene diamin						
61	Frying oil	<10	Degradation of M.B	Alone	effectively decompose the methylene blue solution	Hydrothermal method	[95]
62	Chemical solutions	3.3	Degradation of RhB	TiO_2	More effective degradation when it composed with TiO_2 (increase degradation rate)	Hydrothermal method	[27]
63	Graphene oxide	4	Degradation of M.B	Alone	The photoelectrons were contributed to valence band electron reduction of molecular oxygen to produce superoxide anion ($\bullet O_2^-$) radical or H_2O_2	Hydrothermal method	[96]
64	Graphene oxide	8	Degradation of M.B in the presence of multilayered graphene quantum dots (GQDs)	Alone	Loose the protons from hydroxyl group that resulting a short-lived intermediate product Leucomethylene blue (LMB).	Hydrothermal method	[97]
65	Chemical solution (hydrogen peroxides,	2	Photo-degradation of methyl orange (MO)	Alone	1.The degradation efficiency of MO was about 31.5%, while, under the same reaction conditions, reduction of MO was nearly 0% when no catalyst was used.	Ultrasonic method	[98]

	glucose and ammonia)				2. At 120 min, degradation efficiency 90%		
66	Soot with nitric acid	1	Photo-degradation of methylene blue (M.B)	Alone	At 90 min, degradation efficiency 96%	Chemical oxidation method	[29]
67	Citric acid and phenylenediamine	2	Photocatalytic degradation of organic dyes under simulated sunlight irradiation.	Alone	Complete degradation of both rhodamine B (RhB) and methylene blue (M.B) was achieved in 150 min by the 2-nm CDs.	Microwave-mediated method	[34]
68	Citric acid	2.5-7	Photocatalytic Degradation of Organic Dyes	Alone	Highly efficient photocatalysts for rhodamine B (RhB) and methylene blue (M.B) degradation.	Hydrothermal method.	[31]

Table A2: The effect of dose on rate and efficiency of degradation during 120 minutes.

Time (min)	M.B			0.267 mg/L			0.4 mg/L			0.53 mg/L			0.667 mg/L		
	C	D %	ln (Co/C)	C	D %	ln (Co/C)	C	D %	ln (Co/C)	C	D %	ln (Co/C)	C	D %	ln (Co/C)
0	1.353	0	0	1.367	0	0	1.233	0	0	1.25	0	0	1.23	0	0
10	1.352	0.07391	0.00074	1.267	7.31529	0.07597	1.201	2.5953	0.0263	1.166	6.72	0.06956	1.184	3.73984	0.03812
20	1.256	7.16925	0.07439	1.205	11.8508	0.12614	1.083	12.1655	0.12972	1.062	15.04	0.16299	1.115	9.34959	0.09816
30	1.19	12.0473	0.12837	1.132	17.1909	0.18863	0.974	21.0057	0.23579	0.938	24.96	0.28715	0.954	22.439	0.25411
40	1.023	24.3902	0.27958	0.956	30.0658	0.35762	0.858	30.4136	0.3626	0.818	34.56	0.42404	0.812	33.9837	0.41527
50	1.009	25.425	0.29336	0.873	36.1375	0.44844	0.751	39.0916	0.4958	0.722	42.24	0.54887	0.68	44.7154	0.59268
60	0.989	26.9032	0.31339	0.782	42.7944	0.55852	0.648	47.4453	0.64331	0.603	51.76	0.72898	0.572	53.4959	0.76563
70	0.989	26.9032	0.31339	0.684	49.9634	0.69242	0.557	54.8256	0.79464	0.444	64.48	1.03507	0.425	65.4472	1.06268
80	0.987	27.051	0.31541	0.599	56.1814	0.82511	0.445	63.9092	1.01913	0.388	68.96	1.16989	0.312	74.6341	1.37177
90	0.985	27.1988	0.31744	0.511	62.6189	0.984	0.324	73.7226	1.33646	0.308	75.36	1.4008	0.234	80.9756	1.65945
100	0.985	27.1988	0.31744	0.445	67.447	1.1223	0.287	76.7234	1.45772	0.251	79.92	1.60545	0.199	83.8211	1.82146
110	0.984	27.2727	0.31845	0.427	68.7637	1.16359	0.253	79.4809	1.58382	0.215	82.8	1.76026	0.176	85.6911	1.94429
120	0.982	27.4205	0.32049	0.418	69.4221	1.18489	0.236	80.8597	1.65337	0.192	84.64	1.8734	0.165	86.5854	2.00882
Rate (1/min)	0.01026			0.011			0.01385			0.0166			0.02067		

Table A3: The effect of pH on rate and efficiency of degradation during 120 minutes.

Time (min)	pH 3.8			pH 7			pH 10.6		
	C	D %	ln (Co/C)	C	D %	ln (Co/C)	C	D %	ln (Co/C)
0	1.179	0	0	1.23	0	0	1.171	0	0
10	1.087	7.80322	0.08125	1.184	3.73984	0.03812	0.951	18.7874	0.2081
20	1.098	6.87023	0.07118	1.115	9.34959	0.09816	0.635	45.7728	0.61199
30	1.094	7.2095	0.07483	0.954	22.439	0.25411	0.282	75.918	1.42371
40	1.065	9.66921	0.10169	0.812	33.9837	0.41527	0.165	85.9095	1.95967
50	1.04	11.7897	0.12545	0.68	44.7154	0.59268	0.114	90.2647	2.32941
60	0.996	15.5216	0.16867	0.572	53.4959	0.76563	0.107	90.8625	2.39278
70	0.939	20.3562	0.22761	0.425	65.4472	1.06268	0.106	90.9479	2.40217
80	0.845	28.3291	0.33309	0.312	74.6341	1.37177	0.103	91.2041	2.43088
90	0.795	32.57	0.39408	0.234	80.9756	1.65945	0.103	91.2041	2.43088
100	0.668	43.3418	0.56813	0.199	83.8211	1.82146	0.103	91.2041	2.43088
110	0.525	55.4707	0.80902	0.176	85.6911	1.94429	0.103	91.2041	2.43088
120	0.425	63.9525	1.02033	0.165	86.5854	2.00882	0.103	91.2041	2.43088
Rate (1/min)	0.001189			0.02067			0.06066		

Table A4: The effect of NaCl salt concentrations on rate and efficiency of degradation during 120 minutes.

Time (min)	0 mg			2 mg			4 mg			8 mg		
	C	D %	ln (Co/C)	C	D%	ln (Co/C)	C	D%	ln (Co/C)	C	D %	ln (Co/C)
0	1.23	0	0	1.24	0	0	1.253	0	0	1.322	0	0
10	1.184	3.73984	0.03812	1.074	13.3871	0.14372	1.081	13.7271	0.14765	1.143	13.5401	0.14549
20	1.115	9.34959	0.09816	1.027	17.1774	0.18847	1.018	18.755	0.2077	1.045	20.9531	0.23513
30	0.954	22.439	0.25411	0.931	24.9194	0.28661	0.917	26.8156	0.31219	0.93	29.652	0.35172
40	0.812	33.9837	0.41527	0.753	39.2742	0.4988	0.784	37.4302	0.46889	0.792	40.0908	0.51234
50	0.68	44.7154	0.59268	0.672	45.8065	0.61261	0.652	47.9649	0.65325	0.675	48.941	0.67219
60	0.572	53.4959	0.76563	0.544	56.129	0.82392	0.5	60.0958	0.91869	0.568	57.0348	0.84478
70	0.425	65.4472	1.06268	0.448	63.871	1.01807	0.385	69.2737	1.18005	0.449	66.0363	1.07988
80	0.312	74.6341	1.37177	0.368	70.3226	1.21478	0.276	77.9729	1.5129	0.341	74.2057	1.35502
90	0.234	80.9756	1.65945	0.269	78.3065	1.52816	0.202	83.8787	1.82503	0.259	80.4085	1.63007
100	0.199	83.8211	1.82146	0.19	84.6774	1.87584	0.175	86.0335	1.96851	0.178	86.5356	2.00512
110	0.176	85.6911	1.94429	0.153	87.6613	2.09243	0.161	87.1508	2.05189	0.098	92.587	2.60193
120	0.165	86.5854	2.00882	0.14	88.7097	2.18122	0.102	91.8595	2.50832	0.082	93.7973	2.78018
Rate 1/min	0.02067			0.01712			0.01493			0.01472		

Table A5: The effect of distance on rate and efficiency of degradation during 120 minutes.

Time (min)	0.667mg/L @ 10 cm			0.667mg/L @ 5 cm		
	C	D %	ln (Co/C)	C	D %	ln (Co/C)
0	1.23	0	0	0.933	0	0
10	1.184	3.73984	0.03812	0.899	3.64416	0.03712
20	1.115	9.34959	0.09816	0.729	21.865	0.24673
30	0.954	22.439	0.25411	0.566	39.3355	0.49981
40	0.812	33.9837	0.41527	0.436	53.269	0.76076
50	0.68	44.7154	0.59268	0.319	65.8092	1.07321
60	0.572	53.4959	0.76563	0.242	74.0622	1.34947
70	0.425	65.4472	1.06268	0.18	80.7074	1.64545
80	0.312	74.6341	1.37177	0.141	84.8875	1.88965
90	0.234	80.9756	1.65945	0.118	87.3526	2.06772
100	0.199	83.8211	1.82146	0.101	89.1747	2.22328
110	0.176	85.6911	1.94429	0.093	90.0322	2.30581
120	0.165	86.5854	2.00882	0.086	90.7824	2.38406
Rate (1/min)	0.02067			0.02435		

Table A6: The effect of light source on rate and efficiency of degradation during 120 minutes.

Time (min)	50 W			10 W		
	C	D %	ln (Co/C)	C	D %	ln (Co/C)
0	1.23	0	0	1.164	0	0
10	1.184	3.73984	0.03812	1.118	3.95189	0.04032
20	1.115	9.34959	0.09816	1.106	4.98282	0.05111
30	0.954	22.439	0.25411	1.086	6.70103	0.06936
40	0.812	33.9837	0.41527	1.074	7.73196	0.08047
50	0.68	44.7154	0.59268	1.062	8.76289	0.09171
60	0.572	53.4959	0.76563	1.047	10.0515	0.10593
70	0.425	65.4472	1.06268	1.034	11.1684	0.11843
80	0.312	74.6341	1.37177	1.021	12.2852	0.13108
90	0.234	80.9756	1.65945	1.012	13.0584	0.13993
100	0.199	83.8211	1.82146	1	14.0893	0.15186
110	0.176	85.6911	1.94429	0.989	15.0344	0.16292
120	0.165	86.5854	2.00882	0.979	15.8935	0.17309
Rate (1/min)	0.02067			0.00121		

Table A7: The effect of amounts of pollutant (M.B) on rate and efficiency of degradation during 120 minutes.

Time (min)	35µM M.B			23.3µM M.B			17.5 µM M.B		
	C	D%	ln (Co/C)	C	D%	ln (Co/C)	C	D%	ln (Co/C)
0	1.23	0	0	0.773	0	0	0.668	0	0
10	1.184	3.73984	0.03812	0.652	15.6533	0.17023	0.607	9.13174	0.09576
20	1.115	9.34959	0.09816	0.56	27.555	0.32234	0.536	19.7605	0.22015
30	0.954	22.439	0.25411	0.419	45.7956	0.61241	0.331	50.4491	0.70217
40	0.812	33.9837	0.41527	0.237	69.3402	1.18222	0.189	71.7066	1.26254
50	0.68	44.7154	0.59268	0.149	80.7245	1.64633	0.131	80.3892	1.62909
60	0.572	53.4959	0.76563	0.108	86.0285	1.96815	0.104	84.4311	1.8599
70	0.425	65.4472	1.06268	0.102	86.8047	2.02531	0.098	85.3293	1.91932
80	0.312	74.6341	1.37177	0.101	86.934	2.03516	0.095	85.7784	1.95041
90	0.234	80.9756	1.65945	0.09	88.3571	2.15047	0.093	86.0778	1.97169
100	0.199	83.8211	1.82146	0.089	88.4864	2.16164	0.09	86.5269	2.00448
110	0.176	85.6911	1.94429	0.09	88.3571	2.15047	0.083	87.5749	2.08545
120	0.165	86.5854	2.00882	0.09	88.3571	2.15047	0.075	88.7725	2.1868
Rate (1/min)	0.02067			0.04299			0.05212		

Table A8: The effect of CQDs/ZnO on rate and efficiency of degradation during 120 minutes.

Time (min)	ZnO			CNDs / ZnO		
	C	D %	ln (Co/C)	C	D %	ln (Co/C)
0	1.819	0	0	1.539	0	0
10	1.355	25.5085	0.29449	1.32	14.23	0.1535
20	1.182	35.0192	0.43108	1.186	22.937	0.26055
30	1.07	41.1765	0.53063	1.063	30.9292	0.37004
40	1.006	44.6949	0.5923	0.953	38.0767	0.47927
50	0.928	48.983	0.67301	0.837	45.614	0.60906
60	0.876	51.8417	0.73068	0.736	52.1767	0.73766
70	0.818	55.0302	0.79918	0.655	57.4399	0.85425
80	0.789	56.6245	0.83528	0.595	61.3385	0.95033
90	0.78	57.1193	0.84675	0.553	64.0676	1.02353
100	0.747	58.9335	0.88998	0.452	70.6303	1.22521
110	0.711	60.9126	0.93937	0.323	79.0123	1.56124
120	0.7	61.5173	0.95496	0.288	81.2865	1.67593
Rate (1/min)	0.0072			0.012		